

Tanzania Journal of Science 45(1): 53-66, 2019 ISSN 0856-1761, e-ISSN 2507-7961  
© College of Natural and Applied Sciences, University of Dar es Salaam, 2018

## Performance of a Customized Cryo-Cooling System Designed for the Measurement of the Lifetime of Nuclear Excited States at Cryogenic Temperatures

Innocent J. Lugendo

*Department of Physics, University of Dar es Salaam, P.O Box 35063, Dar es Salaam, Tanzania*

*E-mail address: [ilugendo26@gmail.com](mailto:ilugendo26@gmail.com)*

---

### Abstract

Theoretical predictions that the lifetime of nuclear excited states can be varied if the nucleus is subjected to a condition that allows multiple coherent emission and re-absorption of gamma photons by the nucleus is of much interest to the nuclear physicists. Therefore, an experiment has been designed to study the possibility of lifetime variation. Based on the theory requirements, lifetime variations can be observed when the nucleus is cooled to cryogenic temperatures. Both the cryo-cooling system and the fast timing system have been developed. In the current work, the design, operation and performance of the developed cryo-cooling system is discussed. Furthermore, the effect of operating the cryo-cooling system on the gamma detection system was also studied. The cooling system has been observed to be capable of cooling the radioactive source down to 38 K. Temperature fluctuations of only 0.128% of the selected temperature were observed. This indicates the desired stability of the cooling system. On the other hand, both energy and timing resolution of the detection system were found to be affected by the mechanical vibrations of the cooling system. The effect can be reduced by cushioning the detectors and the remaining minor differences in time resolution can be accounted in the experimental uncertainty budget.

---

**Keywords:** Cryogenic temperature, Cryo-cooling System, Nuclear State, Lifetime Variation, Fast Timing System, Detectors.

### Introduction

The lifetime of a nuclear excited state is an important parameter that is useful in understanding the underlying structure of the nucleus. Determining the lifetime of a nuclear state enables one to derive the state's transition probability (Régis 2011). The transition probability in turn provides information on enhancement and hindrances of the state decay in the evolution of the nuclear structure with a variable number of valence nucleons (Mach et al. 1989). Moreover, these observables are linked with the quantum numbers used as labels for representing the dynamical groups so as to generate the model dependent energy spectrum as well as the nuclear selection

rules and their strengths (Régis et al. 2010). Therefore, the lifetime of a nuclear state provides a direct insight into the structure of the nucleus. It is for this reason that, measurement of the lifetime of the nuclear state is one of the stringent methods of testing the theoretical models describing the nuclear structure (Roussiere et al. 2011). It is due to these significances that, in nuclear physics, precise measurement of the lifetimes of nuclear excited states is indispensable.

Since the beginning of the nuclear spectroscopy, the lifetime of the nuclear excited state has been believed to be a constant and uncontrollable parameter which is not influenced by the nuclear surrounding (Cheon and Jeong 2005). Nevertheless,

several theoretical studies have suggested the dependence of the lifetimes of the nuclear excited states on the nuclear surrounding (Mazaki and Shimizu 1966, Huh 1999, Liu and Huh 2000). A study conducted on the lifetime of the 23.8 keV excited state of  $^{119\text{m}}\text{Sn}$  showed the variation of lifetime when the excited nucleus was surrounded by similar nuclei in their ground states (Loginov 2010). A handful of studies have established a theory that predicts the variation of the lifetimes of the nuclear excited states under nuclear resonance conditions (Cheon and Jeong 2005). These studies have demonstrated via theoretical calculations and simulations that the mean lifetime of the nuclear state will be prolonged if the emitted gamma photons are coherently reflected and reabsorbed by the decaying nuclei, a phenomenon named as the “Boomerang Effect” (Cheon 2015). However, the predicted variation of lifetime needs to be proved experimentally before the theory can be endorsed. This requires setting an experiment that can observe the lifetimes of nuclear states when subjected to the conditions suggested by the theoretical predictions. One of the important theoretical conditions for the lifetime variation is that, both the decaying nuclei and the gamma reflectors must be kept at cryogenic temperatures to avoid lattice vibrations and the recoiling effects (Cheon and Jeong 2005). Thus, in setting an experiment to observe the variation of lifetimes of nuclear excited states, a cryo-cooling machine that can maintain both the source and the reflectors at cryogenic temperatures is necessary. Moreover, the small value of the predicted change in lifetime means a very precise and accurate lifetime measurement system is required. Therefore, in the efforts to observe the variation of lifetime, this study has paid heed in designing a cryo-cooling system and a precise timing system as the two important parts of the experiment. The aim of the current work is to discuss the design and the performance of the customized cryo-cooling

system developed for the experiment to observe changes in nuclear lifetimes. Furthermore, tests have been conducted to study the effects of mechanical vibrations of the designed cryo-cooling system during its operation on the performance of the fast timing system developed for the lifetime measurements. This paper discusses both the design and performance of the cooling system as well as its influence on the sensitivity of the fast timing system.

## **Materials and Methods**

### **Design of the cooling system**

A customized table size cryo-cooling system was designed for the purpose of cooling the radioactive source to cryogenic temperatures. The system was made of 4 major units which are the vacuum unit, the radioactive source holder, the Sterling engine and the temperature control unit. Figure 1 shows the sketch and picture of the designed cryo-cooling system. Vacuum was created in the small hexagonal vacuum chamber located on the top of the system using a rotary vacuum pump. The chamber was made of 5 mm thick steel walls. On each side of the hexagonal chamber, there was a 1 mm thick quartz window of radius 13 mm. The chamber was designed such that the distance between two opposite quartz windows was 180 mm. A KC 430 MINI SHIM gauge was fixed just beside the vacuum chamber to monitor the pressure inside the chamber. A hollowed rectangular source holder made of copper and coated with gold was firmly attached to the cold cap of the sterling engine and stationed at the centre of the vacuum chamber. The source holder was fabricated using the gold plated copper material so as to improve the thermal stability of the cooler (Dubuis et al. 2014). The holder had a width of 50 mm and length of 60 mm with a thickness of 5 mm. A circular hollow of diameter 30 mm and 30 mm deep was drilled for holding the radioactive source. Both the vacuum chamber and the source holder are displayed in Figure 2.

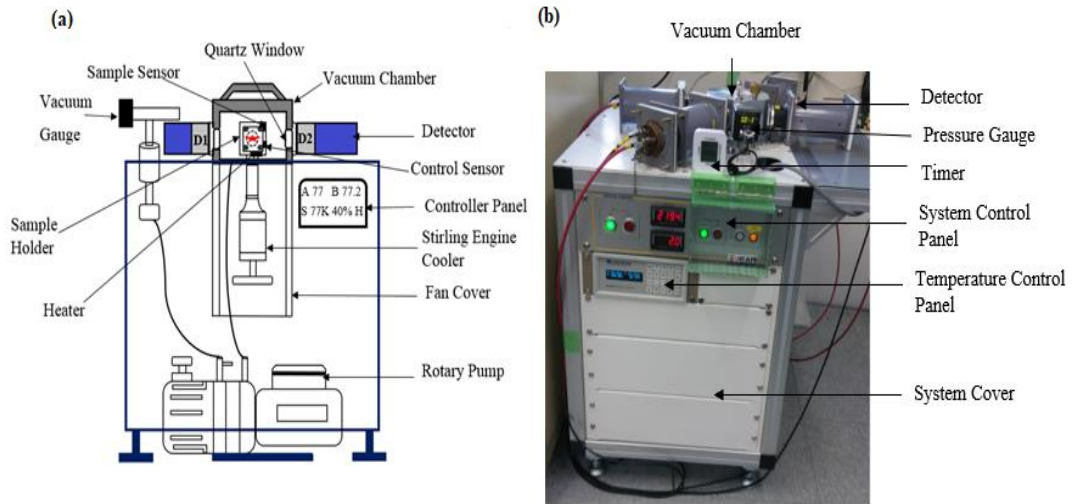


**Figure 1:** (a) Sketch and (b) Picture of the designed cryo-cooling system showing the important parts of the system.

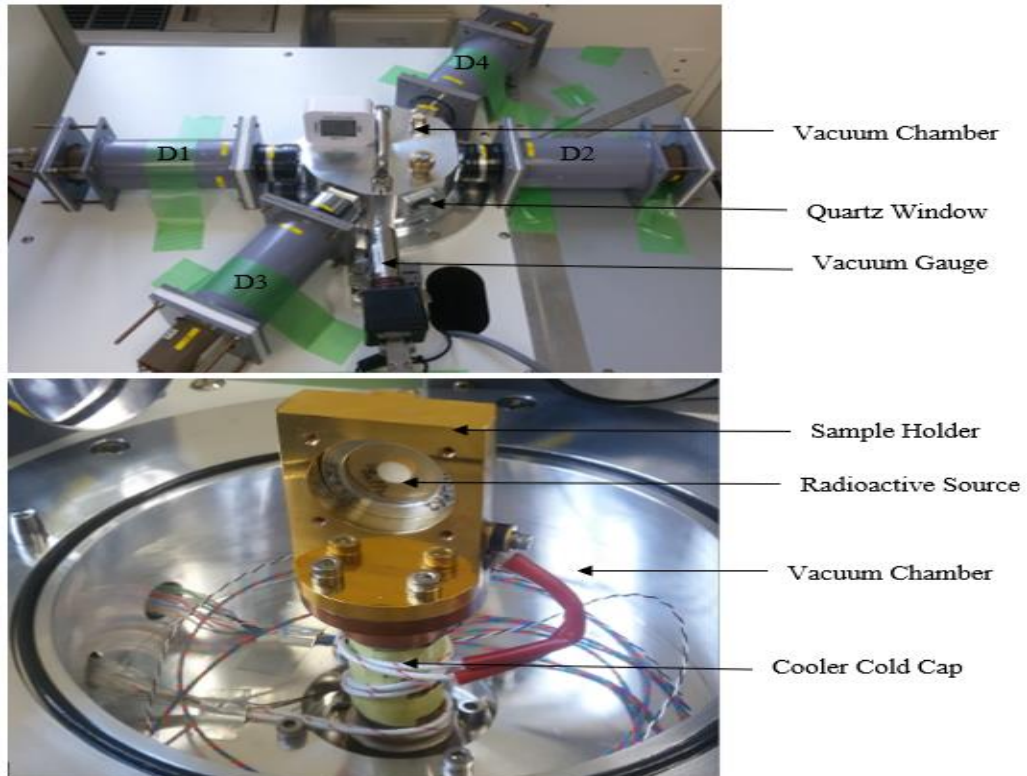


**Figure 2:** Description of the vacuum chamber and the sample holder.

Cooling was made possible by using a single piston Sterling engine whose cold cap was directly coupled to the sample holder. This engine was 276 mm high and weighed 3.1 kg making it fairly portable. The engine was driven using a linear electrical motor with helium as the working gas. Cooling was done through the heat exchange process at the cold fins which were firmly attached to the cold cap via the cold finger. The engine had a power input of 140 W with heat lift of 60 K enabling it to cool the radioactive source to as low as 38 K. A temperature control unit was used to monitor the temperatures of both the cold cap and the radioactive source. The unit was composed of a heater, DT-670 silicon diode temperature sensors and the "Lake Shore" dual channel temperature controller. Using the temperature control unit, the load temperature could be selected in the range of 300 to 38 K enabling measurement of lifetime at different temperatures.

#### The source container

To ensure effective cooling of the radioactive source, a customized steel container was designed to contain the

radioactive source. Steel was chosen due to its high thermal conductivity at low temperatures (Olsen and Rosenberg 1953) and fairly acceptable gamma attenuation coefficient (Buyuk 2015). The container was made of two circular plates of diameter 5 mm and thickness of 5 mm so as to fit in the sample holder of the cooler. On each plate, a cylindrical hollow of diameter 3 mm and 3 mm deep was drilled at the central position of the plate to form a required cylindrical structure (Cheon and Jeong 2005). A 189 kBq  $^{133}\text{Ba}$  source was wrapped in a 50  $\mu\text{m}$  thick polyester film. The film was then sandwiched between the two plates such that the source was in direct contact with the steel plates while enclosed at the centre of the cylindrical hollows. This allows efficient cooling of both the radioactive source and the container. Cooling the source and the container lowers the Debye effect thus enhances the recoilless scattering and re-absorption of the gamma photons (Modest 2013). The plates were held together using small flat headed screws. The design of the source container is shown in Figure 3.

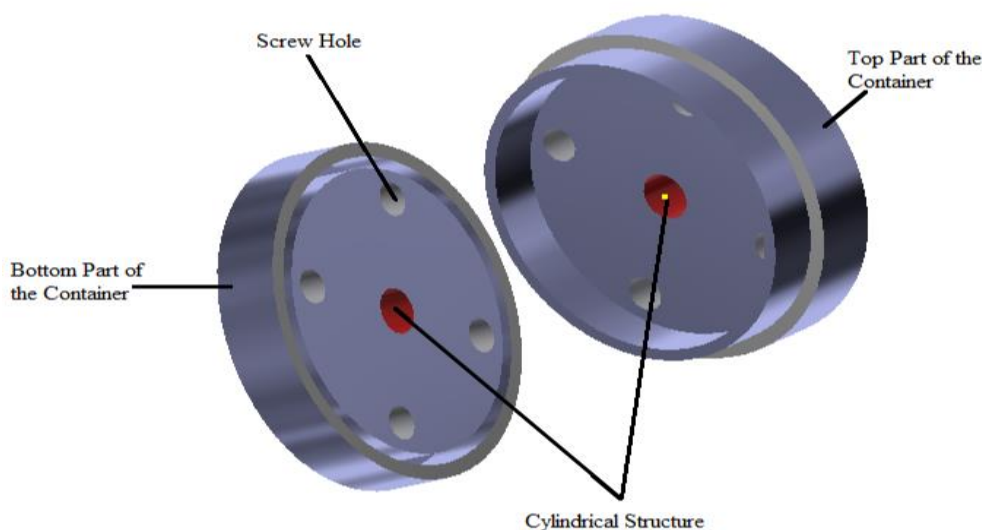


**Figure 3:** A steel container that held the radioactive source during the experiment.

### Performance of the cooling system

Two experiments were performed to study the suitability of the system. One experiment was geared towards measuring temperature and pressure variations with respect to time. The other experiment aimed at assessing the effect of the cooling system on the gamma detection capability. In order to measure temperature and pressure variations of the cooling system, the system was turned on and the output readings of both pressure and temperature were recorded. While temperature was recorded after every 15 minutes, pressure was recorded after every 2 minutes. At first, the temperature was set to 38 K and the cooler was turned “on” while the heater was “off”. The load temperature readings were then recorded until the temperature of 38 K was reached. The cooling system was then left to operate for 15 hours at 38 K. During this time, the radioactive source temperature readings were recorded in the intervals of 30 minutes in order to determine the temperature stability and the discrepancy between the set temperature and the load temperature. After 15 hours, the cooler was switched “off” and the system was allowed to heat up to 300 K for 5 hours. During the heating period, the load temperature readings were recorded at intervals of 5 minutes until the load temperature reached the ambient temperature of 300 K. Meanwhile, pressure in the vacuum chamber was measured after every 2 minutes during the whole time of the experiment.

On the other hand, since the cooling system is mechanical, vibrations caused by the moving parts of the cooling system could affect the gamma detection capability of the detector system (McCabe 2015). Therefore, tests were performed to examine the influence of the vibrations of the cooling system on the energy resolution as well as the time resolution of the gamma detection system. To achieve this, a gamma detection system was set as shown in Figure 4. The detection system comprised of two “2 x 2”

NaI(Tl) detectors which were labelled as D4 and D3, one “1.5 x 1.5” LaBr<sub>3</sub>(Ce) detector labelled as D2 and one “1 x 1” LaBr<sub>3</sub>(Ce) detector labelled as D1. Detectors were arranged such that D1 and D2 faced each other while D3 and D4 faced each other with the radioactive source placed 9 cm from the face of each detector. All detectors were powered by 2 identical NIM power supply modules each having two output channels. The 4 power supply output channels were set to +1047 V, +1125 V, 1438 V and +1260 V for detectors D1, D2, D3 and D4, respectively. From each detector, a signal was split into two signals whereby one signal was fed into the discriminating module and the other was fed into the Analogue to Digital Converter (ADC) - CAMAC module via the delay modules. The discriminated signal from each detector was fed into a coincidence module which generated an output only when at least two signals coincide. A coincidence signal is fed into the gate generating module which generates a 1 microsecond gate signal used to initiate counting in the ADC. Meanwhile, other discriminated signals from each detector were passed through the digital variable delay modules before being fed into the Time to Digital Converter (TDC) as stop signals. The gate signal was used as the common start signal for the TDC. Figure 4 describes the gamma detection system used during this study.

Using this gamma detection system, gamma rays from <sup>133</sup>Ba, <sup>137</sup>Cs and <sup>60</sup>Co radioactive sources were measured first with the cooling system turned “off” and then with the cooling system turned “on”. In both cases, each radioactive source was analysed for 30 minutes. The obtained spectra were all corrected by subtracting the physical background which was mainly due to the activity of <sup>40</sup>K in the surrounding. Peaks of various dominant gamma lines were fitted to Gaussian functions and the centroid and width parameters of the fit functions were recorded. Finally, the energy resolution of a

given detector at a particular gamma energy was computed by using equation 1 (Lugendo

2017). This procedure was done for each detector that builds the detection system.

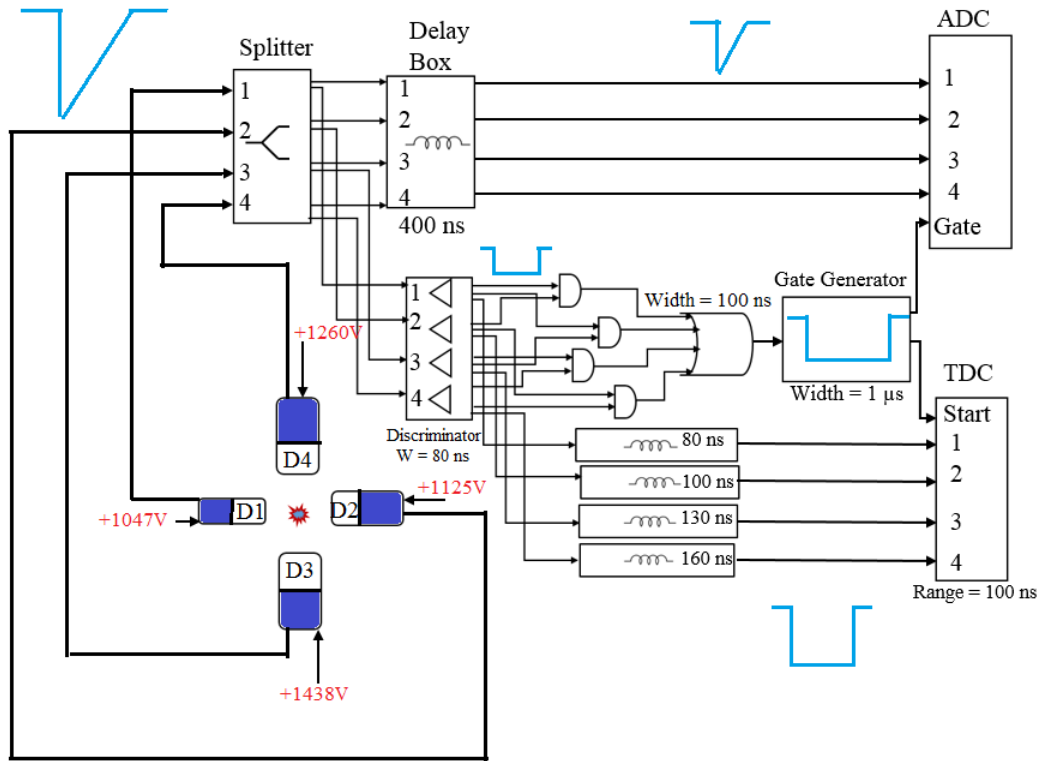


**Figure 4:** The gamma detection system. Detectors arrangement as well as the electronic data readout circuit are displayed.

$$R(\%) = \frac{2.35\sigma}{\mu} \times 100\% \quad (1)$$

where, R is the energy resolution

$\sigma$  is the width of the Gaussian function

$\mu$  is the centroid of the Gaussian function

Besides the energy resolution capability of the detection system, it was also important to study the time resolution capability of the system. The 1173 keV and 1332 keV gamma lines from the beta decay of  $^{60}\text{Co}$  to  $^{60}\text{Ni}$  at ground state were used to measure the time resolution of the detection system. To achieve such a measurement, gamma spectrum from the decay of  $^{60}\text{Co}$  source was recorded for 10 hours. Data obtained were sorted out such

that tri-dimensional coincidence matrices were developed using different pairs of detectors. The matrices were labelled M ( $E_X, E_Y, T_{X-Y}$ ) whereby the first axis represents the energy measured by the one detector, X and the second axis represents the energy measured by the second detector, Y. The third axis represents the time difference between the detector signals with X and Y, respectively acting as the Start and Stop

signals of a “Common Start” Time to Digital Converter (TDC) module deployed for this study. The energy gates for the two detectors were set such that signal X was the 1173 keV gamma line while signal Y was the 1332 keV gamma line. For instance, for the D1nD2 combination, detector D1 was set to view the 1173 keV line and the detector D2 was set to view the 1332 keV gamma line. Since the lifetime of the 1333 keV state of  $^{60}\text{Ni}$  is 0.713 ps (Be' et al. 2006) which is too short, the time difference between X and Y in this case is merely a Gaussian distribution representing the Prompt Response Function (PRF) of the detection system (Lugendo 2017). This PRF can be used to estimate the time resolution of the employed detector combination. This was done by first correcting the Time Difference Spectrum (TDS) by subtracting the time walk effect as well as the Compton background. Then, the corrected TDS was fitted to the Gaussian function that was developed using ROOT V.5.4. This procedure was carried out for the four detector combinations that showed best spectra from this experiment. These combinations were labelled D1nD2, D1nD3, D2nD4 and D3nD4. The time resolution for each detector combination was estimated by using the width of the corresponding Gaussian function (Regis et al. 2010).

Like in the case of energy resolution, in order to determine the effect of the cooling system on timing resolution of the detection system, time resolution was measured when the source was inside the vacuum chamber with the cooling system turned “off”.

Subsequently, the timing resolution was re-measured when the source was inside the vacuum chamber with the cooling system operating at the temperature of 38 K. Results obtained from the two sets of measurements for both energy resolution and time resolution were compared in order to discern the effect of the cooling system on the gamma detection capability.

### Results and Discussion

Observation of the temperature variations with time, revealed the capacity of the cooling system. The rates of the temperature variations when the cooling system is operating are described in Figure 5. It took approximately 60 minutes for the radioactive source to be cooled from the ambient temperature to 38 K, about 300 minutes elapsed as the source was heated from 38 K to 300 K. While the rate of cooling for this system was found to be comparable to the rate of cooling reported in other studies (Sosso et al. 2018), the rate of heating was considerably slow. The slower rate of heating of this system is an advantage for this study as the lifetime measurement is to be performed at cryogenic temperature for long periods of time. Moreover, it shows the goodness of the system design in terms of heat transfer. Data points were fitted to some empirical equations using ROOT V. 5.4. The fitting equations are displayed in Figure 5 and may be used to accurately predict the cooling and heating process of this cooling system.

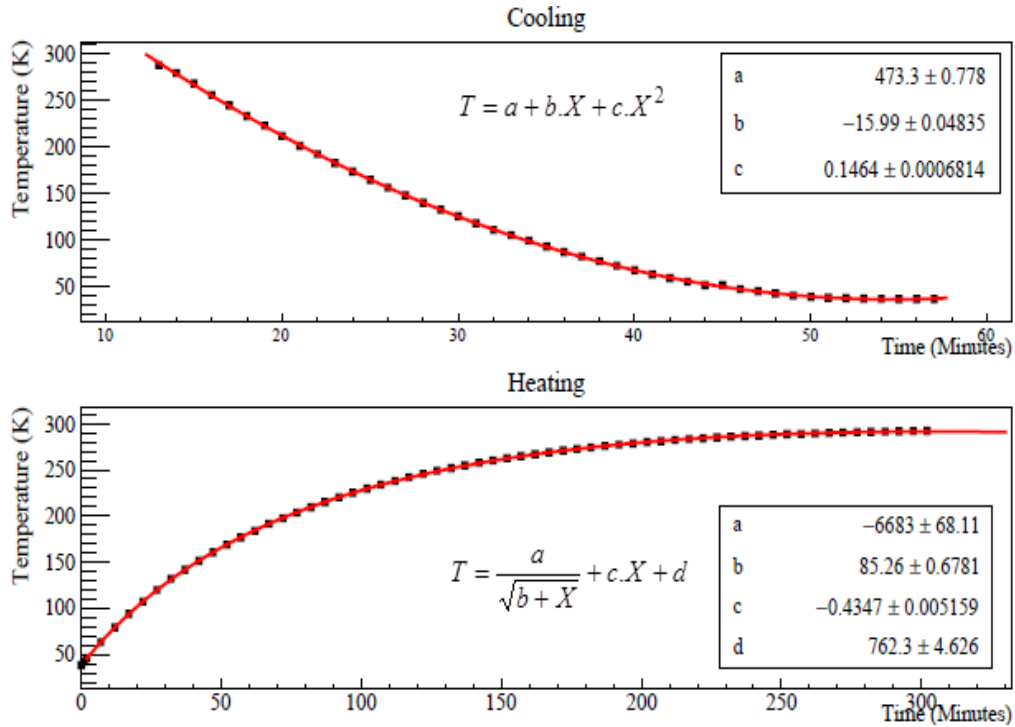


**Figure 5:** Temperature variations of the radioactive source. The top figure shows the cooling process while the bottom figure shows the heating process. The line represents the fitting equation that can be used to model the load temperature variations.

Furthermore, by using the data recorded in a period of 15 hours, temperature stability of the load was evaluated. It was observed that the load temperatures recorded in steps of 30 minutes during the period of 15 hours spanned between 38.04 and 38.06 K. This is described in Figure 6. The average load temperature was found to be 38.049 K with a standard deviation of 0.003 K. The standard deviation was taken as the error in load temperature value and it was only 0.007 % of the average recorded load temperature. As one of the major challenges in designing a cryocooling system is the temperature stability (Sosso et al. 2018), the results from this experiment reveal the brilliance of the designed cooling system in terms of the temperature stability. The temperature

stability of this system is attributed to the use of the gold plated copper sample holder as gold helps to increase the thermal capacitance of holder (Dubuis et al. 2014). On the other hand, as the system was set to cool the load to 38 K, the average discrepancy between the set cooler temperature and the actual load temperature was observed to be 0.049 K which is 0.128% of the cooler set temperature. This shows the ability of this cooling system to cool its load to the desired temperature and maintain the temperature with satisfactorily minimum fluctuations. Hence, the cooler was confirmed to be capable of accurately cooling the radioactive source to the desired temperatures and maintaining the set temperature for the whole period of lifetime measurement.

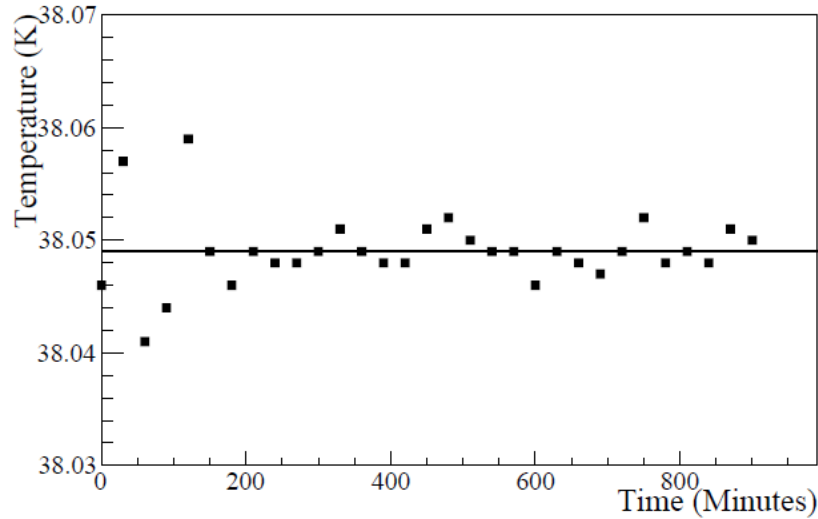


**Figure 6:** A scatter plot showing the distribution of the load temperature over time during 15 hours of the experiment. The squares represent the temperature values while the line shows the average recorded load temperature.

Besides the temperature variations, the readings recorded to study the vacuum system showed that it takes 15 minutes for the pressure inside the vacuum chamber to fall to about  $1 \times 10^{-4}$  Torr. This pressure was

observed to be maintained over the whole period of the cooling system operation as displayed in Figure 7. Therefore, the vacuum system was observed to be performing well for the purpose of the designed experiment.

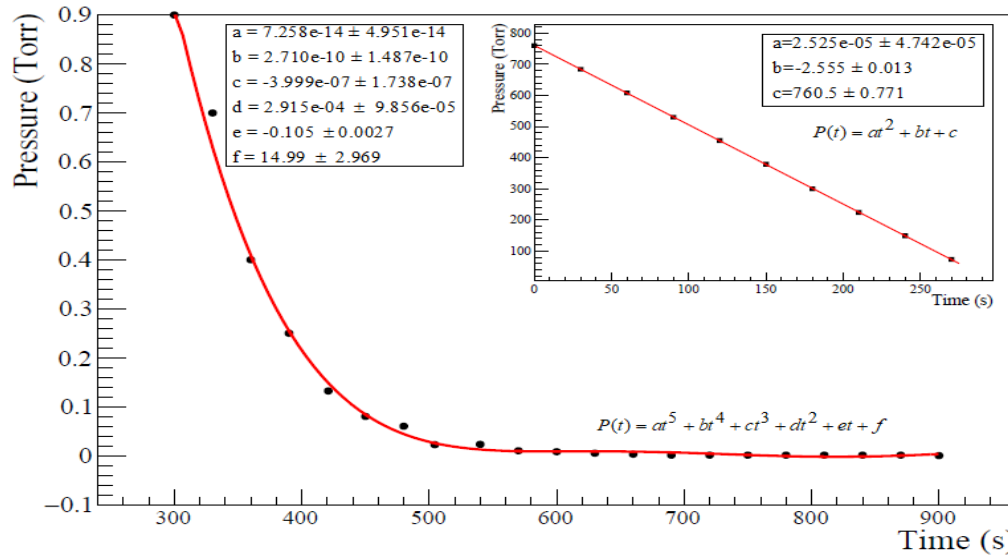


**Figure 7:** Pressure variations in the vacuum chamber after the vacuum pump is switched on. The inserted figure shows the variation from the ambient pressure to 760 Torr whereas the main figure illustrates the pressure variation down to 0.001 Torr.

On the other hand, both energy and time resolutions of the detection system were assessed for the sake of understanding how the gamma detection system is affected by the operation of the cooling system. Gamma spectra from  $^{60}\text{Co}$ ,  $^{133}\text{Ba}$  and  $^{137}\text{Cs}$  radioactive sources were recorded first when the cooling

system was turned “off”. Then these measurements were repeated with the cry-cooling system operating at 38K. Figure 8 displays the gamma spectra recorded by individual detectors when the cry-cooling system was not operating.

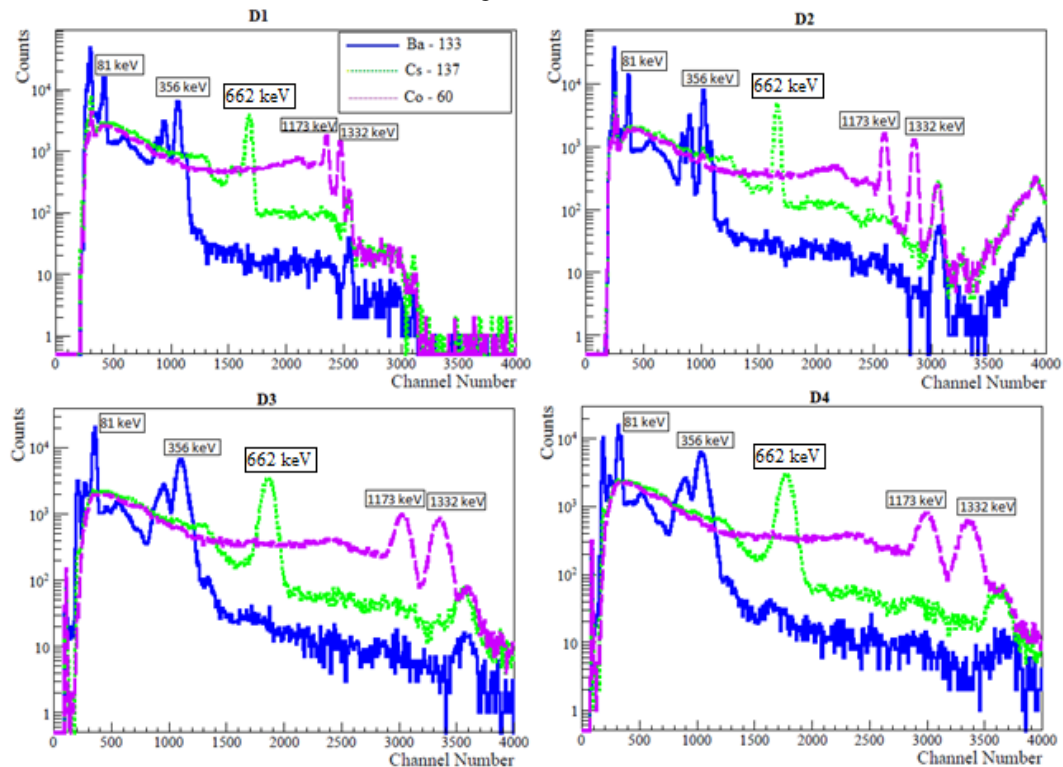


**Figure 8:** Gamma spectra from  $^{133}\text{Ba}$ ,  $^{137}\text{Cs}$  and  $^{60}\text{Co}$  sources as recorded by each of the 4 detectors when the cooling system was switched “off”.

Energy resolution for each detector was determined at the 81 keV, 356 keV, 662 keV, 1173 keV and 1332 keV gamma peaks. Each peak was fitted to the Gaussian function and the energy resolution at that particular gamma energy was calculated using equation 1. The energy resolution at each gamma energy was re-measured from the spectra recorded when the cooling system was operating. Finally, comparison of energy resolution at each gamma peak for the two

states of the cooling system were compared as described by Figure 9.

As it can be observed from Figure 9, comparison between energy resolutions reveals that the resolutions at all measured gamma lines for all detectors tend to increase when the cooling system is operating. The average increases in the energy resolutions were observed to be 0.25 % for D1, 1.4% for D2, 1.5% for D3 and 1.7% for D4. Since all the detectors were rested on top of the

cooling system, the increase in the energy resolutions is assumed to arise from the vibrations due to moving parts of the cooling system. Nevertheless, the average increases in D2, D3 and D4 are seen to be comparable while the increase in D1 is very small. This observation is attributed to the fact that D1

was the smallest detector and it was positioned using some fibres in order to make its height comparable to other detectors. The fibre seemed to act as the shock absorber and hence reduced the effect of vibrations to this detector.

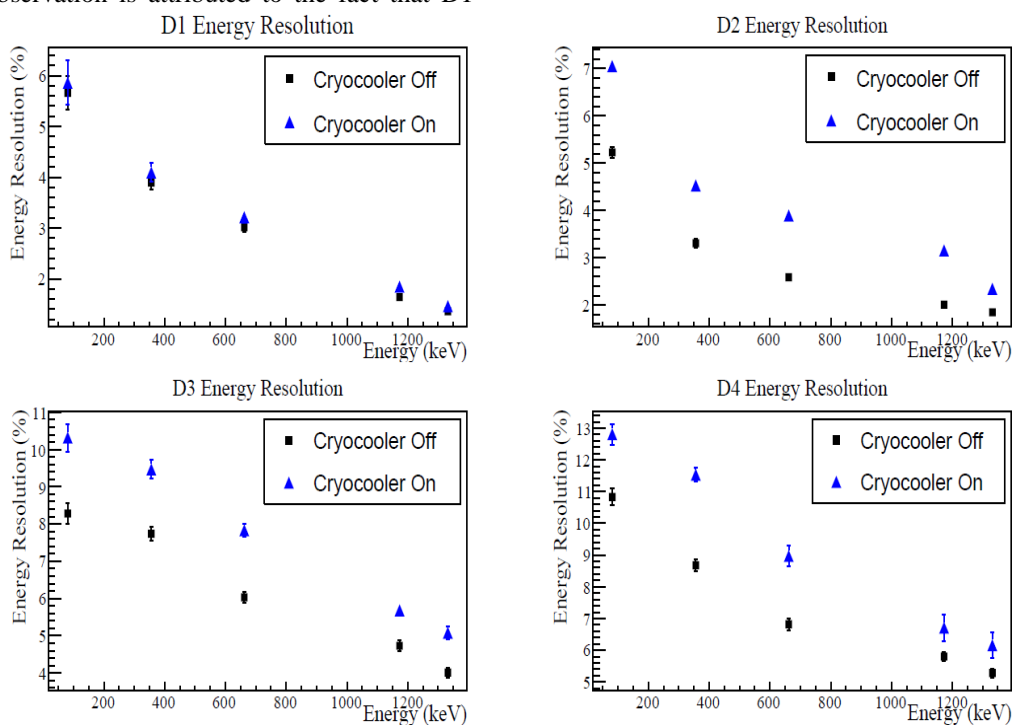


**Figure 9:** Comparison of energy resolution measured when the cryo-cooler was “off” and when the cryo-cooler was operating at 38 K.

Furthermore, the time difference spectrum from the 1173 keV and 1332 keV gamma lines was measured when the cryocooler was switched “off” and then re-measured when the cryo-cooler was operating at 38 K. Figure 10 shows the time difference spectra recorded from different selected detector combinations when the cryocooler was switched “off”.

The time difference spectrum from each detector combination was fitted with a Gaussian function as shown by a solid red line in Figure 10. For each detector combination, the sigma ( $\sigma$ ) value of the Gaussian function that produced the best fit

was used to estimate the time resolution of the respective detector combination. Same procedure was repeated in order to determine the time resolution for the same detector combinations when the cryo-cooler was operating at 38 K. Results obtained from the two cases were compared to observe the effect of the cryo-cooling system on the timing resolution of the detection system. The comparison of time resolution measured with the cryo-cooling system switched “off” and with the cooling system operating at 38 K is displayed in Figure 11.

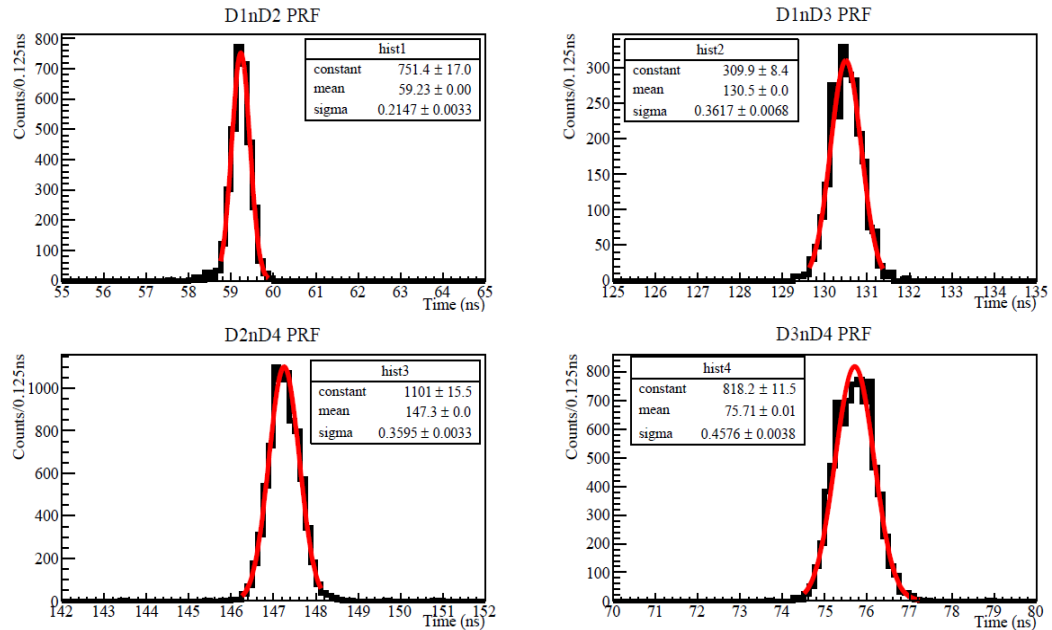


**Figure 10:** Time resolution of the detection system measured using four different detector combinations. The histogram shows the time distribution while the smooth curve line is the Gaussian function used to fit the data.

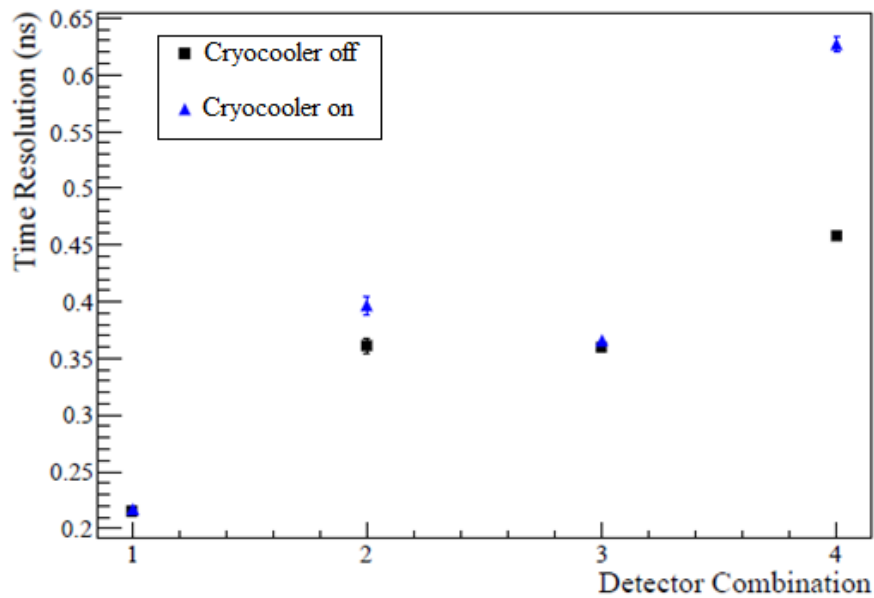


**Figure 11:** Comparison of the energy resolutions measured when the cryo-cooler was “off” and when the cryo-cooler was operating at 38 K. Numbers 1, 2, 3 and 4 represent the detector combinations D1nD2, D1nD3, D2nD4 and D3nD4, respectively.

While the effect of the cryocooler vibrations on time resolutions was observed to be insignificant for the detector combinations D1nD2 and D2nD3, the effect was much vivid for the detectors combinations D1nD3 and D3nD4. The difference in time resolution for D1nD3 was attributed to the fact that D3 was larger than D1 and was experiencing more vibrations as the Sterling engine operated. These vibrations affect the energy resolution by widening the peak widths and consequently allow noises underneath the signal when selecting the region of interest (ROI). Meanwhile, both D3 and D4 are NaI(Tl) detectors which are known to have great gamma detection efficiency but comparably poor energy resolution. The energy resolution of NaI(Tl) detectors is even worse when the detectors are subjected to mechanical vibrations as is the case of Sterling engine operation. Therefore, the huge difference in time resolution for the combination D3nD4 is of no surprise. In the effort to reduce the effect of mechanical vibrations on the energy and timing resolution of the gamma detection system, special cushions were made to support the detectors. The cushions reduced the fluctuation in time resolution by about 60% and the remaining differences were accounted for in the uncertainty budget of the detection results.

### Conclusion

In this work, the design as well as the performance of the cryo-cooling system that has been developed to enable measurements of nuclear lifetimes at cryogenic temperatures have been discussed. The system uses the Sterling engine to cool the radioactive source down to 38 K. The system is also embedded with an electrical heater and an electronic temperature selector that enhances the selection of temperature in the range of 38 K to 100 K. The performance of the cryo-system has been tested by studying the temperature and pressure variations during

the operation. It was found that the system can cool the radioactive source down to 38 K in about 60 minutes. The stability of the system was also probed, and only minor temperature fluctuations were observed in the period of 15 hours of the experiment, indicating sufficient stability of the cooling system. Furthermore, as the cryo-cooling system employs the Sterling engine, the influence of the mechanical vibrations on the gamma detection system was studied. It was observed that both the energy and time resolution of the detection system were affected by the mechanical vibrations due to the operation of the cooling system. These effects were reduced by cushioning the detectors and the remaining slight discrepancies can be accounted in the uncertainty budget.

### Acknowledgement

The author acknowledges the efforts put to this work by Jung K. Ahn, Byungsik Hong and all other members of the Nuclear and High Energy Physics Laboratory at Korea University. The author is also thankful to the Physics Department of the Korea University for hosting the experiments at the HANUL Laboratory.

### References

- Buyuk B 2015 Gamma attenuation behaviour of some stainless and boron steels. *Acta Phys. Polon. A* 127(4): 1342–1345.
- Be' MM, Chiste V, Dulieu C, Browne E, Baglin C, Chechev V, Kuzmenco N, Helmer R, Kondev F, MacMahon D, Lee KB 2006 Table of Radionuclides vol. 3 - A = 3 to A = 244, Bureau International des Poids et Mesures, Pavillon de Breteuil, France, pp. 23–28.
- Cheon IT 2015 Physics behind modification of the nuclear lifetime by the  $\gamma$ -ray boomerang effect. *Phy. Sci. Int. J.* 5(1): 12–17

- Cheon IT and Jeong MT 2005 Measurement of the nuclear lifetime altered by two parallel plates. *JKPS* 46(2): 397–400.
- Dubuis G, Xi H and Bozovic I 2014 Sub millikelvin sytabilization of a closed cycle cryocooler. *Rev. Sci. Instr.* 85: 1–11.
- Huh CA 1999 Dependence of the decay rate of  $^7\text{Be}$  on chemical forms. *Earth Planet. Sci. Lett.* 171(3): 325–328.
- Liu L and Huh CA 2000 Effect of pressure on the decay rate of  $^7\text{Be}$ . *Earth Planet. Sci. Lett.* 180(1): 163–167.
- Loginov YE 2010 Change in the observed half-life of an excited nuclear state under conditions of a resonance environment. *Phys. Atom. Nucl.* 73(1): 34–37.
- Lugendo IJ 2017 *Possible change in lifetime of the first excited state of  $^{133}\text{Cs}$  in a metal reflector at low temperature*. PhD thesis, Korea University.
- Mach H, Gill RL and Moszyński M 1989 A method for picosecond lifetime measurements for neutron-rich nuclei, *Nucl. Instr. Methods A* 280(1): 49–72.
- Mazaki H, Shimizu S 1966 Effect of chemical state on the decay constant of  $^{235}\text{U}$ . *Phy. Rev.* 148(3): 1161–1167.
- McCabe JB 2015 *Characterization of mechanically cooled High Purity Germanium (HPGE) detectors at elevated temperatures*. PhD thesis, University of Tennessee, Knoxville.
- Modest MF 2013 Radiative Properties of Real Surfaces. In: Radiative Heat Transfer vol. 3, Academic Press, Pennsylvania, pp. 61–128.
- Olsen JL and Rosenberg HM 1953 The thermal conductivity of metals at low temperature. *Adv. Phys.* 2(5): 28–66.
- Régis JM 2011 *Fast Timing with  $\text{LaBr}_3(\text{Ce})$  Scintillators and the mirror symmetric centroid difference method*. PhD Thesis, University of Cologne.
- Régis JM, Pascovici G, Jolie J, Rudigier M 2010 The mirror symmetric centroid difference method for picosecond lifetime measurements via  $\gamma$ - $\gamma$  coincidences using very fast  $\text{LaBr}_3(\text{Ce})$  scintillator detectors. *Nucl. Instr. Methods A* 622(1): 83–92.
- Roussiere B, Cardona MA, Deloncle I, Hojman D, Kiener J, Petkov P, Venkova T 2011 Half-life measurements of  $^{137}\text{Cs}$ ,  $^{139}\text{Cs}$  excited nuclear states. *Eur. Phys. J. A-Hadr. Nucl.* 47(9): 1–14.
- Sosso A and Durandetto P 2018 Experimental analysis of the thermal behaviour of a CM cryocooler based on linear system theory. *Int. J. Refrig.* 92: 125–132.